

Aberystwyth University

Frictionless Motion of Lattice Defects

Gorbushin, N.; Mishuris, G.; Truskinovsky, L.

Published in:

Physical Review Letters

DOI:

[10.1103/PhysRevLett.125.195502](https://doi.org/10.1103/PhysRevLett.125.195502)

Publication date:

2020

Citation for published version (APA):

Gorbushin, N., Mishuris, G., & Truskinovsky, L. (2020). Frictionless Motion of Lattice Defects. *Physical Review Letters*, 125(19), [195502]. <https://doi.org/10.1103/PhysRevLett.125.195502>

General rights

Copyright and moral rights for the publications made accessible in the Aberystwyth Research Portal (the Institutional Repository) are retained by the authors and/or other copyright owners and it is a condition of accessing publications that users recognise and abide by the legal requirements associated with these rights.

- Users may download and print one copy of any publication from the Aberystwyth Research Portal for the purpose of private study or research.
- You may not further distribute the material or use it for any profit-making activity or commercial gain
- You may freely distribute the URL identifying the publication in the Aberystwyth Research Portal

Take down policy

If you believe that this document breaches copyright please contact us providing details, and we will remove access to the work immediately and investigate your claim.


tel: +44 1970 62 2400
email: is@aber.ac.uk

Frictionless Motion of Lattice Defects

N. Gorbushin,¹ G. Mishuris^{1,2}, and L. Truskinovsky¹

¹*PMMH, CNRS—UMR 7636, CNRS, ESPCI Paris, PSL Research University, 10 rue Vauquelin, 75005 Paris, France*

²*Department of Mathematics, Aberystwyth University, Ceredigion SY23 3BZ, Wales, United Kingdom*

 (Received 22 June 2020; revised 24 September 2020; accepted 24 September 2020; published 2 November 2020)

Energy dissipation by fast crystalline defects takes place mainly through the resonant interaction of their cores with periodic lattice. We show that the resultant effective friction can be reduced to zero by appropriately tuned acoustic sources located on the boundary of the body. To illustrate the general idea, we consider three prototypical models describing the main types of strongly discrete defects: dislocations, cracks, and domain walls. The obtained control protocols, ensuring dissipation-free mobility of topological defects, can also be used in the design of metamaterial systems aimed at transmitting mechanical information.

DOI: [10.1103/PhysRevLett.125.195502](https://doi.org/10.1103/PhysRevLett.125.195502)

Mobile crystalline defects respond to lattice periodicity by dynamically adjusting their core structure which leads to radiation of lattice waves through parametric resonance [1–5]. Such purely conservative dumping is one of the main mechanisms of energy loss for fast-moving dislocations [6,7], crack tips [8,9], and elastic phase or twin boundaries [10,11]. Similar effective dissipation hinders the mobility of topological *defects* in mesoscopic dispersive systems, from periodically modulated composites [12] to discrete acoustic metamaterials [13].

While at the macroscale friction is usually diminished by applying lubricants, at the microscale it may be preferable to use instead external sources of ultrasound (sonolubricity) [14]. Correlated mechanical vibrations are also known to reduce macroscopic friction through acoustic unjamming [15] as in the case of the remote triggering of earthquakes [16]. Similarly, more general detachment front tips can be viewed as macroscopic defects whose mobility in highly inhomogeneous environments can be controlled by ac (alternating current) driving [17]. Ultrasound-induced lubricity is even more relevant for the reduction of friction at the microscale [18]. It is known, for instance, that the forming load drops significantly in the presence of appropriately tuned time-periodic driving affecting dislocation friction [19].

The ac-based control of the directed transport in *damped* systems was studied extensively in the case when the sources are distributed in the bulk [20–22]. In this Letter, we neglect the conventional damping, associated, for instance, with “phonon wind” [23], and show how in a purely Hamiltonian setting the effective friction can be tuned to zero by the special ac driving placed on the system boundary [24,25].

Since classical continuum models lack the resolution to describe dynamic defect cores and, therefore, cannot capture adequately the interaction between a defect and external microstructure, we use atomistic model which accounts for

the coupling between the defect and the lattice vibrations while respecting the anharmonicity of interatomic forces. We build upon the theoretical methodology developed in Refs. [10,26,27] and show that ac driving can compensate radiative damping *completely*, making the discrete system fully transparent for mobile topological defects.

To highlight ideas, we present a comparative study of the three snapping-bond-type lattice models originating in crystal plasticity [Frenkel-Kontorova (FK) model [7]], theory of structural phase transitions [bistable Fermi-Pasta-Ulam (FPU) model [28]], and fracture mechanics [Peyrard-Bishop (PB) model [29]].

In the individual setting of each of these models, we study the effect of the boundary ac sources on mobility laws for the corresponding lattice defects. The latter relate the macroscopic driving force (dynamic generalization of the Peach-Koehler force in the case of dislocations, the stress intensity factor in the case of cracks, and the Eshelby force in the case of phase boundaries) to the velocity of the defect. We find that in the presence of ac sources such relations become continuously *multivalued*. We focus particularly on designing the ac protocols which ensure that the steady propagation of a defect takes place under zero driving force.

In addition to applications in conventional materials science, the possibility of externally guided radiation-free propagation of mechanical information is presently of considerable interest for designing discrete metamaterials with buckling linkages. Geometric phase transitions generating information-carrying defects in such systems play a central role in a multitude of new applications from recoverable energy harvesting to controlled structural collapse [30–32].

The FPU model with bistable interactions will be used to represent the simplest crystal defect, a *domain wall* [11,33]. In terms of dimensionless particle displacements $u_j(t)$, the dynamics is described by the system

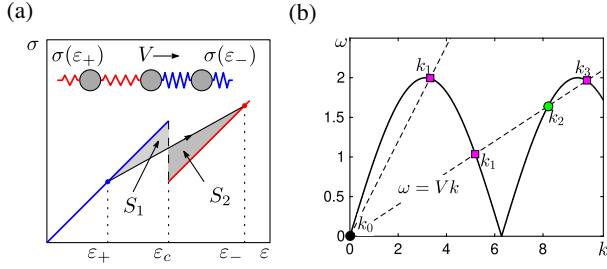


FIG. 1. (a) Piecewise linear stress-strain relation $\sigma = \sigma(\epsilon)$; the macroscopic driving force $G^M(V) = S_2 - S_1$. (b) Dispersion relation $\omega(k)$ for $\text{Im}(k) = 0$ (acoustic branch); k_j correspond to the radiated waves in cases $K = 1$ and $K = 3$; see the text. Green circles correspond to ac sources behind the defect, and magenta squares ahead of the defect.

$$\ddot{u}_j(t) = \sigma(u_{j+1} - u_j) - \sigma(u_j - u_{j-1}). \quad (1)$$

It will be convenient to use strain variables $\epsilon_j(t) = u_{j+1}(t) - u_j(t)$ and introduce the strain energy density $w(\epsilon)$ so that $\sigma(\epsilon_j) = w'(\epsilon_j)$. For analytical transparency, we adopt the simplest biquadratic model with $w = (1/2)\epsilon^2 - \sigma_0(\epsilon - \epsilon_c)H(\epsilon - \epsilon_c)$, where $H(x)$ is the Heaviside function, ϵ_c is the characteristic strain, and σ_0 is the stress drop; see Fig. 1(a).

We search for traveling wave (TW) solutions of Eq. (1) in the form $u_j(t) = u(\eta)$, where $\eta = j - Vt$ and $V < 1$ is the normalized velocity of the defect. If we associate the defect with $\eta = 0$, the equation for the strain field reduces to $V^2 d^2 \epsilon / d\eta^2 = \sigma(\eta + 1) + \sigma(\eta - 1) - 2\sigma(\eta)$, where $\sigma(\eta) = \epsilon(\eta) - \sigma_0 H(-\eta)$. When this linear equation is solved, the velocity V is found from the nonlinear switching condition $\epsilon(0) = \epsilon_c$.

Using the Fourier transform $\hat{f}(k) = \int_{-\infty}^{\infty} f(\eta) e^{ik\eta} d\eta$, we can rewrite the main linear problem in the form $L(k)\hat{\epsilon}(k) = \sigma_0 \omega^2(k)/(0 + ik)$, where $L(k) \equiv \omega^2(k) - (kV)^2$ and $\omega^2(k) = 4 \sin^2(k/2)$ is the dispersion relation represented by a single acoustic branch; see Fig. 1(b). The strain field $\epsilon(\eta)$ can be decomposed into a sum of the term $\epsilon_{\text{in}}(\eta)$, which is due to inhomogeneity (mimicking non-linearity) and the term $\epsilon_{\text{dr}}(\eta)$, due to the combined action of dc (direct current) and ac driving. The former can be written explicitly

$$\epsilon_{\text{in}}(\eta) = \frac{\sigma_0}{2\pi} \int_{-\infty}^{\infty} \frac{\omega^2(k) e^{-ik\eta}}{(0 + ik)L(k)} dk. \quad (2)$$

The latter must satisfy $L(k)\hat{\epsilon}_{\text{dr}}(k) = 0$, which in the physical space gives

$$\epsilon_{\text{dr}}(\eta) = \sum_{j=1}^K A_j \sin(k_j \eta + \varphi_j) + C. \quad (3)$$

The constants A_j and φ_j describe the amplitude and the phase, respectively, of the incoming waves generated at the distant boundaries. They represent the ac driving which is

characterized by the wave numbers k_j that are taken among the positive real roots of the kernel $L(k)$; if $\omega'(k_j)$ is smaller (greater) than V , the sources are in front of (behind) the moving defect. The constant C in (3), representing the root $k_0 = 0$, controls the uniform strain ahead of the moving defect and describes the dc driving.

Using the switching condition, we can obtain the explicit relations for the limiting strains in the form $\langle \epsilon \rangle(\pm\infty) \equiv \epsilon_{\pm} = \epsilon_c \mp \frac{1}{2}(\sigma_0/1 - V^2) + \sigma_0 Q - \sum_{j=1}^K A_j \sin \varphi_j$, where $\langle f \rangle = \lim_{T \rightarrow \infty} (1/T) \int_0^T f(s) ds$; the expression for the universal function $Q(V)$ can be found in Ref. [34]. It can be checked that the obtained solution respects the macroscopic momentum balance represented by the Rankine-Hugoniot (RH) condition [39]: $V^2 = [\sigma(\epsilon_+) - \sigma(\epsilon_-)] / (\epsilon_+ - \epsilon_-)$. The limiting values of the mass velocity $v_j = \dot{u}_j$ automatically satisfy another (kinematic) RH condition $\langle v \rangle(\pm\infty) \equiv v_{\pm} = -V\epsilon_{\pm}$.

We now write the macroscopic energy dissipation on the moving defects as $\mathcal{R} = VG \geq 0$, where G is the driving force. In the absence of the ac driving ($A_j = 0$), we obtain $G = G^M$, where

$$G^M = \llbracket w \rrbracket - \{ \sigma \} \llbracket \epsilon \rrbracket, \quad (4)$$

and we used the standard notations $\llbracket f \rrbracket = f_+ - f_-$ and $\{ f \} = (f_+ + f_-)/2$ [40]. In our case, $G^M = (\sigma_0/2)(\epsilon_+ + \epsilon_- - 2\epsilon_c)$. With the ac driving present, we obtain $\mathcal{R} = V(G^M + G^m) \geq 0$, where the total power exerted by microscopic sources is

$$VG^m = \sum_{j=1}^K (1/2) A_j^2 |\omega'(k_j) - V| \geq 0. \quad (5)$$

The implied relation for \mathcal{R} can be checked by the independent computation of the energy carried by the microscopic radiation away from the moving defect [34].

The dependence of $G = G^M + G^m$ on V for a high-velocity subset of admissible solutions is shown in Fig. 2(a). The radiative damping is represented here by a single wave number k_1 . The ac driving is tuned to the same wave number, and its source is placed ahead of the moving defect (the $K = 1$ regime). If the ac driving is absent and all $A_j = 0$, there is a single value of V for each value of G within the admissible range $\pm[\epsilon_c - \epsilon(\eta)] > 0$ at $\pm\eta > 0$. Even if only one coefficient $A_1 \neq 0$, each admissible value of velocity V can be reached within a finite range of dc driving amplitudes with the associated phase shift φ_1 varying continuously. In this sense, the conventional singlevalued *kinetic relation* transforms into a 2D *kinetic domain* [see Fig. 2(a)], where by fixing the strength of dc drive we can either speed up or slow down the defect as we change the frequency of the ac source.

The possibility of the ac-induced friction *reduction* is seen from the fact that for each V there is a range of the admissible driving forces $G < G(A_1 = 0)$ with the minimal

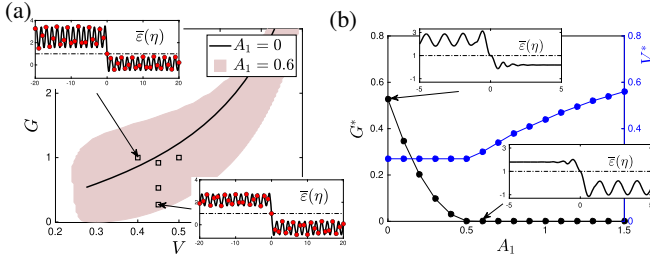


FIG. 2. (a) Kinetic domain for the case $K = 1$; open squares show the selected TW solutions reached numerically [34]. (b) Amplitude dependence of G^* and V^* ; insets show normalized strains $\bar{\varepsilon}(\eta) = \varepsilon(\eta)/\varepsilon_c$. Parameters: $\sigma_0 = 2$ and $\varepsilon_c = 1$.

value $G^*(V)$. Moreover, for some V^* , such friction can be eliminated completely if the amplitude A_1 reaches beyond a threshold. We remark that the emergence of friction-free regimes resembles a second-order phase transition with the dissipation G^* as the order parameter; see Fig. 2(b) and Ref. [34], where we compute the corresponding critical exponent. The nondissipative regimes with $K = 1$ are naturally antiphase with respect to the radiated waves so that $\varphi_1^* = \pi/2$; see a typical strain distribution in the insets in Fig. 2(b). The relation between the ac amplitude and the defect velocity for such regimes can be written explicitly $A_1^* = \sigma_0 V / [V - \omega'(k_f)]$.

In the general case $K \neq 1$, the number of dissipative waves is odd, and the dissipation-free regimes also must have an odd number of ac sources to cancel each of these waves. Consider, for instance, the case $K = 3$, illustrated in Fig. 1(b), where two dissipative lattice waves (k_1 and k_3) release energy at $-\infty$ and one wave (k_2) at $+\infty$. To block these dissipative waves, one must have the sources of ac driving both in front and behind the defect. The corresponding amplitudes, ensuring that $G^*(V) = 0$, are $A_j^* = (-1)^j \sigma_0 V / [\omega'(k_j) - V]$ with $j = 1, 2, 3$; see Ref. [34] for details.

Our numerical checks suggest that the admissible frictionless regimes exist only for $K = 1$. To show stability of the frictionless solutions, we performed numerical experiments using Eq. (3) as an initial condition. The nonstationary problem was solved while the ends of the chain were kept free, meaning that $\ddot{\varepsilon}_1 = \sigma(\varepsilon_2) - 2\sigma(\varepsilon_1)$ and $\ddot{\varepsilon}_N = \sigma(\varepsilon_{N-1}) - 2\sigma(\varepsilon_N)$. The snapshots of the emerging steady front are shown in Fig. 3; the transient stage is illustrated in Supplemental Movie 1 [34].

While our construction above was based on the biquadratic model, allowing complete analytical transparency, the TW problem can be also solved semianalytically in the case of a smoother, three-parabola potential containing a spinodal region; see [34] for details.

The simplest FK model [6,41] can be used to study the frictionless propagation regimes of a moving *dislocation*; see Fig. 4(a). If we deal with a single dislocation, it is sufficient to use only two wells of the on-site periodic potential. The displacement $u_j(t)$, describing horizontal slip, must solve the equations

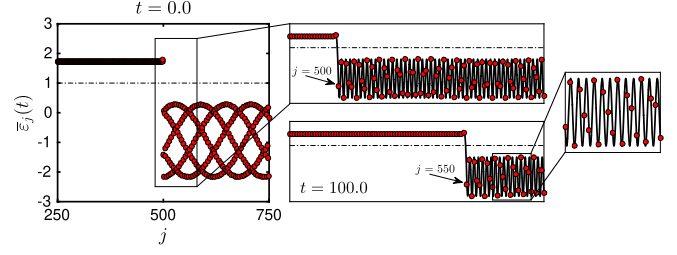


FIG. 3. Steady propagation of the phase transition front obtained numerically for a finite chain with $N = 1000$ starting from the initial data (3) with $V = 0.5$. Normalized strain $\bar{\varepsilon}_j(t) = \varepsilon_j(t)/\varepsilon_c$ is shown at three different moments of time. The inset shows a comparison with the analytical TW solution (solid line).

$$\ddot{u}_j = u_{j-1} + u_{j+1} - 2u_j - \sigma(u_j) + \tau, \quad (6)$$

where τ is a uniform load. The corresponding piecewise linear function $\sigma(u)$ is illustrated in Fig. 4(a). It is defined via the on-site potential $w(u) = (1/2)u^2$ when $-u_c < u < u_c$ and $w(u) = (1/2)u^2 - \sigma_0(u - u_c)$ when $u_c < u < 3u_c$, representing the two relevant periods. We again use the TW ansatz $u_j(t) = u(\eta)$, $\eta = j - Vt$ and apply the same condition of admissibility. Unlike the previous case, the dc drive τ is now applied in the bulk.

We need to solve the linear equation $V^2 u''(\eta) = u(\eta+1) + u(\eta-1) - 3u(\eta) + \sigma_0 H(-\eta) + \tau$ and then find the defect velocity V using the nonlinear condition $u(0) = u_c$. The solution can be again represented in the form $u(\eta) = u_{\text{in}}(\eta) + u_{\text{dr}}(\eta)$. The first term, which is due to inhomogeneity (mimicking nonlinearity), now includes the dc driving τ :

$$u_{\text{in}}(\eta) = \tau + \frac{\sigma_0}{2\pi} \int_{-\infty}^{\infty} \frac{e^{-ik\eta}}{(0+ik)L(k)} dk, \quad (7)$$

where the operator $L(k)$ remains the same as in the FPU problem but the dispersion relation $\omega^2(k) = 4\sin^2(k/2) + 1$ is now represented by a single optical branch. The second term responsible for the ac driving must satisfy $L(k)\hat{u}_{\text{dr}}(k) = 0$ and can be again represented as a combination of linear waves whose phase velocity is equal to V :

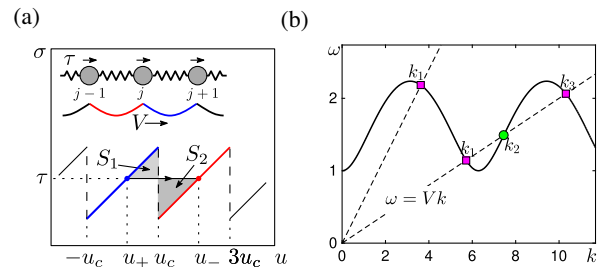


FIG. 4. (a) Dislocation propagation driven by the constant force τ ; macroscopic driving force $G^M(V) = S_2 - S_1$. (b) Dispersion relation for $\text{Im}(k) = 0$ (optical branch). The wave numbers k_j define radiated waves in the cases $K = 1$ and $K = 3$.

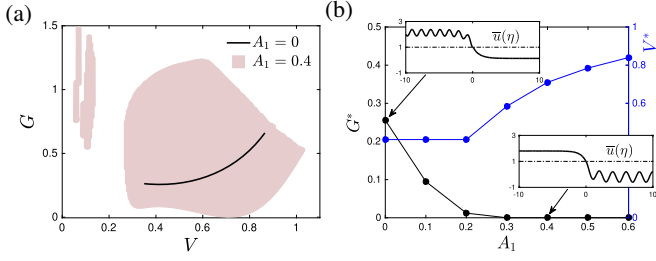


FIG. 5. (a) Kinetic domains for dislocations showing admissible solutions with $K = 1$. There is only one damping wave in the big pink domain and more than one in the smaller ones. (b) The ac amplitude dependence of $G^*(V^*)$ and V^* ; insets show displacements $\bar{u}(\eta) = u(\eta)/u_c$. Parameters: $\sigma_0 = 2$ and $u_c = 1$.

$$u_{dr}(\eta) = \sum_{j=1}^K A_j \sin(k_j \eta + \varphi_j). \quad (8)$$

Here k_j are again the positive real roots of $L(k) = 0$.

Using the switching condition, we obtain for the time-averaged displacements at $\pm\infty$ the values $u_{\pm} = u_c \mp (\sigma_0/2) + \sigma_0 R - \sum_j A_j \sin \varphi_j$ with the explicit expression for the universal function $R(V)$ given in Ref. [34]. The analogs of the RH conditions are now $u_+ = \tau$ and $u_- = \tau + \sigma_0$.

If we denote the stress in the horizontal bonds by $\bar{\sigma}(\varepsilon) = \varepsilon$, we can write the rate of dissipation at the macroscale as $VG^M = \llbracket v^2/2 + \varepsilon^2/2 + w - \tau u \rrbracket V + \llbracket \bar{\sigma} v \rrbracket$. Applying the kinematic RH condition $\llbracket v \rrbracket + V \llbracket \varepsilon \rrbracket = 0$, we obtain

$$G^M = \llbracket w \rrbracket - \tau \llbracket u \rrbracket. \quad (9)$$

Since $\varepsilon_{\pm} = \bar{\sigma}(\varepsilon_{\pm}) = 0$, we can finally write the macroscopic driving force in the form $G^M = \sigma_0^2/2 - \sigma_0(u_c - u_+)$. The contribution to the energy flux due to ac sources is now

$$VG^m = \sum_{j=1}^K (1/2) A_j^2 \omega^2(k_j) |\omega'(k_j) - V| \geq 0. \quad (10)$$

The continuously multivalued relation $\mathcal{R}(V) = VG(V) = G^M(V) + G^m(V)$ for admissible solutions is illustrated in Fig. 5(a) for the case $K = 1$. It is again possible to completely cancel the lattice friction and obtain regimes with $G^*(V^*) = 0$. In such regimes, illustrated for $K = 1$ in Fig. 5(b), the radiated waves are annihilated by the waves generated by the ac source with the amplitudes $A_j^* = (-1)^j \sigma_0 V / \{\omega(k_j)^2 [\omega'(k_j) - V]\}$ and phase shifts $\varphi_j^* = \pi/2$; see Ref. [34] for details.

Our last example deals with reversible *fracture* in the simplest PB-type setting [9,29,42]. The lattice defect is now a crack tip moving under the action of a transversal force (from left to right) by consequently breaking the bonds represented by elastic fuses; see Fig. 6(a).

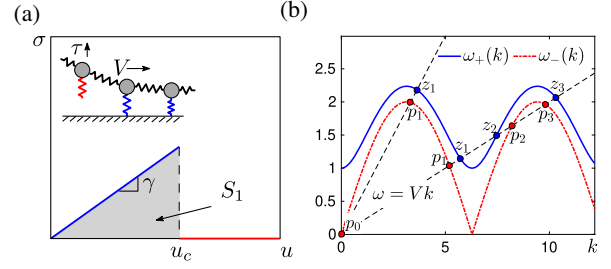


FIG. 6. (a) Constitutive relation for a mechanical fuse and schematic representation of a crack propagating with velocity V under remote load τ ; the strain energy jump $\llbracket w \rrbracket = -S_1$. (b) Dispersion relations $\omega_+(k)$ (optical branch) and $\omega_-(k)$ (acoustic branch) for $\text{Im}(k) = 0$ characterizing intact and broken lattices, respectively.

The equations governing the evolution of the vertical displacements $u_j(t)$ are

$$\ddot{u}_j = u_{j-1} + u_{j+1} - 2u_j - \gamma u_j H(u_j - u_c); \quad (11)$$

see Fig. 6(a) for notations—and we again look for solutions in the TW form $u_j(t) = u(\eta)$, $\eta = j - Vt$. We need to solve a linear equation $V^2 u''(\eta) = u(\eta + 1) + u(\eta - 1) - 2u(\eta) - \gamma u(\eta) H(\eta)$ and use the nonlinear switching condition $u(0) = u_c$ to find the defect velocity V . The dispersion relations are now represented by one optical branch $\omega_+^2(k) = 4 \sin^2(k/2) + \gamma$ ahead of and one acoustic branch $\omega_-^2(k) = 4 \sin^2(k/2)$ behind the defect.

One way to solve this more complex problem is to use the Wiener-Hopf technique; see Ref. [34] for details. We can again obtain the decomposition $u(\eta) = u_{in}(\eta) + u_{dr}(\eta)$, but now to define the two additive terms we need to introduce two auxiliary functions $L^{\pm}(k) = L^{\mp 1/2}(k) \exp(1/2\pi i \int_{-\infty}^{\infty} \text{Log} L(\xi)/(k - \xi) d\xi)$, where $L(k) \equiv [\omega_+^2(k) - (kV)^2]/[\omega_-^2(k) - (kV)^2]$. Then

$$u_{in}(\eta) = \frac{C}{2\pi} \int_{-\infty}^{\infty} \frac{L^{\pm}(k) e^{-ik\eta}}{0 \mp ik} dk, \quad \pm \eta > 0, \quad (12)$$

is the contribution due to remotely applied dc force τ which is modeled by the condition that at $\eta = -\infty$ the time average displacements follows the asymptotics $u(\eta) \sim -\tau\eta$; we also assumed here that at $\eta = +\infty$ the average displacement tends to zero. From these conditions we find that $C = \tau S \sqrt{(1 - V^2)/\gamma}$ where an explicit expression for the function $S(V)$ is given in Ref. [34]. The contribution due to the ac driving is

$$u_{dr}(\eta) = \frac{1}{2\pi} \int_{-\infty}^{\infty} L^{\pm}(k) \Psi_{dr}^{\pm}(k) e^{-ik\eta} dk, \quad \pm \eta > 0, \quad (13)$$

where

$$\Psi_{dr}^{\pm}(k) = \sum_{j=1}^K \frac{A_j}{2} \left[\frac{e^{-i(\varphi_j - \pi/2)}}{0 \mp i(k - k_j)} + \frac{e^{i(\varphi_j - \pi/2)}}{0 \mp i(k + k_j)} \right]. \quad (14)$$

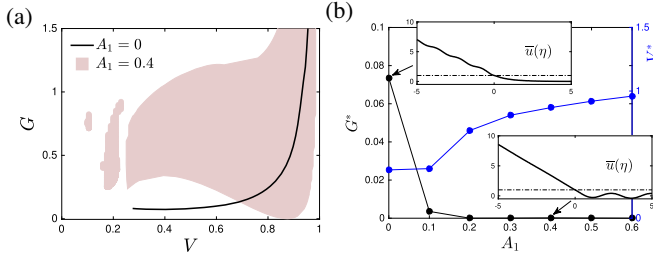


FIG. 7. (a) Kinetic domains for admissible solutions with $K = 1$ and the ac wave coming from ahead. There is only one damping wave in the big pink domain and more than one in the smaller ones. (b) Amplitude dependence of $G^*(V^*)$ and V^* . Material properties are $\gamma = 1$ and $u_c = 1$.

Here the wave numbers $k_j = z_{2j-1}$ describe the sources bringing the energy from $+\infty$, while the wave numbers $k_j = p_{2j}$ correspond to sources bringing the energy from $-\infty$; for the cases $K = 1, 3$, the wave numbers z and p are illustrated in Fig. 6(b).

To compute the driving force G^M , we observe that the macroscopic energy dissipation on the crack tip is $VG^M = \llbracket v^2/2 + \varepsilon^2/2 + w \rrbracket V + \llbracket \bar{\sigma}v \rrbracket$, where $w(u) = (1/2)\gamma u^2$ for $u < u_c$ and $w(u) = (1/2)\gamma u_c^2$ for $u > u_c$. If we now take into consideration the RH condition $\llbracket v \rrbracket + V \llbracket \varepsilon \rrbracket = 0$, we obtain $VG^M = \llbracket w \rrbracket V + \tilde{f} \{v\}$. Here $\tilde{f} = \llbracket \bar{\sigma} \rrbracket - V^2 \llbracket \varepsilon \rrbracket$ is the moving concentrated force, which represents the microscopic processes in the tip and also secures that the linear momentum RH condition is satisfied; see, e.g., Ref. [43]. We can now write

$$G^M = \llbracket w \rrbracket - \tilde{f} \llbracket \varepsilon \rrbracket, \quad (15)$$

and, substituting the values $\varepsilon_- = -\tau$, $\varepsilon_+ = 0$, $\bar{\sigma}(\varepsilon_{\pm}) = \varepsilon_{\pm}$, we finally obtain $G^M = \tau^2(1 - V^2)/2 - (\gamma u_c^2)/2$.

Consider the simplest case when there is only one radiated wave with $k_1 = p_1$. The microscopic power exerted by a single ac source ahead of the crack ($K = 1$) is then

$$VG^m = \frac{1}{2} A_1^2 \omega_+^2(z_1) |L^+(z_1)|^2 |\omega_+(z_1) - V| \geq 0. \quad (16)$$

The total dissipation $\mathcal{R}(V) = VG(V) = V[G^M(V) + G^m(V)] \geq 0$ is again a multivalued function of V as we show in Fig. 7(a); the associated functions $G^*(V^*)$ and V^* at different values of A_1 are shown in Fig. 7(b). At a given V we obtain $A_1^* = u_c(z_1^2 - p_1^2)/z_1^2$, $\varphi_1^* = \pi/2$, and the corresponding dissipation-free solution is illustrated in the inset in Fig. 7(b). Solutions with $K > 1$ are discussed in Ref. [34].

In conclusion, we showed that it is possible to fine tune defect kinetics by carefully engineered ac driving. Moreover, using special ac sources on the boundary, one can compensate radiative damping completely, making the crystal free of internal friction for strongly discrete defects.

We demonstrated this effect for domain boundaries, dislocations, and cracks; however, the obtained results also have important implications for the design of artificial metamaterials supporting mobile topological defects and capable of transporting compact units of mechanical information.

The authors thank L. Slepyan for helpful discussions. This work was supported by EPSRC Grant No. EP/R014604/1. N.G and L.T. also acknowledge the Grant No. ANR-10-IDEX-0001-02 PSL. G.M. acknowledges Royal Society for the Wolfson Research merit Award.

- [1] J. Currie, S. Trullinger, A. Bishop, and J. Krumhansl, *Phys. Rev. B* **15**, 5567 (1977).
- [2] M. Peyrard and M. D. Kruskal, *Physica (Amsterdam)* **14D**, 88 (1984).
- [3] C. Kunz and J. A. Combs, *Phys. Rev. B* **31**, 527 (1985).
- [4] R. Boesch, C. R. Willis, and M. El-Batanouny, *Phys. Rev. B* **40**, 2284 (1989).
- [5] P. G. Kevrekidis, I. G. Kevrekidis, A. R. Bishop, and E. S. Titi, *Phys. Rev. E* **65**, 046613 (2002).
- [6] W. Atkinson and N. Cabrera, *Phys. Rev.* **138**, A763 (1965).
- [7] O. Kresse and L. Truskinovsky, *J. Mech. Phys. Solids* **52**, 2521 (2004).
- [8] L. I. Slepyan, *Dokl. Acad. Nauk*, **258**, 561 (1981); *Doklady Soviet Phys.* **26**, 538 (1981), <http://www.mathnet.ru/links/07f75f9aca894718280445dc90f55b16/dan44473.pdf>.
- [9] M. Marder and S. Gross, *J. Mech. Phys. Solids* **43**, 1 (1995).
- [10] L. I. Slepyan, *J. Mech. Phys. Solids* **49**, 469 (2001).
- [11] L. Truskinovsky and A. Vainchtein, *SIAM J. Appl. Math.* **66**, 533 (2005).
- [12] T. Dohnal, A. Lamacz, and B. Schweizer, *Asymptotic Analysis* **93**, 21 (2015).
- [13] D. M. Kochmann and K. Bertoldi, *Appl. Mech. Rev.* **69**, 050801 (2017).
- [14] V. Pfahl, C. Ma, W. Arnold, and K. Samwer, *J. Appl. Phys.* **123**, 035301 (2018).
- [15] R. Capozza, A. Vannossi, A. Vezzani, and S. Zapperi, *Phys. Rev. Lett.* **103**, 085502 (2009).
- [16] L. de Arcangelis, E. Lippiello, M. Pica Ciamarra, and A. Sarracino, *Phil. Trans. R. Soc. A* **377**, 20170389 (2019).
- [17] S. M. Rubinstein, G. Cohen, and J. Fineberg, *Nature (London)* **430**, 1005 (2004).
- [18] F. Dinelli, S. Biswas, G. Briggs, and O. Kolosov, *Appl. Phys. Lett.* **71**, 1177 (1997).
- [19] C. E. Winsper, G. R. Dawson, and D. H. Sansome, *Met. Mater.* **4**, 158 (1970).
- [20] L. L. Bonilla and B. A. Malomed, *Phys. Rev. B* **43**, 11539 (1991).
- [21] D. Cai, A. R. Bishop, N. Grønbech-Jensen, and B. A. Malomed, *Phys. Rev. E* **50**, R694(R) (1994).
- [22] B. B. Baizakov, G. Filatrella, and B. A. Malomed, *Phys. Rev. E* **75**, 036604 (2007).
- [23] H. Koizumi, H. O. K. Kirchner, and T. Suzuki, *Phys. Rev. B* **65**, 214104 (2002).
- [24] Z. Tshirprut, A. E. Filippov, and M. Urbakh, *Phys. Rev. Lett.* **95**, 016101 (2005).

- [25] R. Capozza, S. M. Rubinstein, I. Barel, M. Urbakh, and J. Fineberg, *Phys. Rev. Lett.* **107**, 024301 (2011).
- [26] G. S. Mishuris, A. B. Movchan, and L. I. Slepyan, *J. Mech. Phys. Solids* **57**, 1958 (2009).
- [27] M. Nieves, G. Mishuris, and L. Slepyan, *Int. J. Solids Struct.* **112**, 185 (2017).
- [28] Y. R. Efendiev and L. Truskinovsky, *Continuum Mech. Thermodyn.* **22**, 679 (2010).
- [29] F. Maddalena, D. Percivale, G. Puglisi, and L. Truskinovsky, *Continuum Mech. Thermodyn.* **21**, 251 (2009).
- [30] S. Shan, S. H. Kang, J. R. Raney, P. Wang, L. Fang, F. Candido, J. A. Lewis, and K. Bertoldi, *Adv. Mater.* **27**, 4296 (2015).
- [31] Y. Zhang, B. Li, Q. Zheng, G. M. Genin, and C. Chen, *Nat. Commun.* **10**, 5605 (2019).
- [32] R. L. Harne and K.-W. Wang, *Harnessing Bistable Structural Dynamics: For Vibration Control, Energy Harvesting and Sensing* (John Wiley & Sons, New York, 2017).
- [33] L. Slepyan, A. Cherkaev, and E. Cherkaev, *J. Mech. Phys. Solids* **53**, 407 (2005).
- [34] See Supplemental Material at <http://link.aps.org/supplemental/10.1103/PhysRevLett.125.195502> for the details of the analytical derivations, the setting of the numerical experiments, and the study of the role of the spinodal region in the FPU problem, which includes Refs. [11,35–38].
- [35] N. Flytzanis, S. Crowley, and V. Celli, *J. Phys. Chem. Solids* **38**, 539 (1977).
- [36] A. Vainchtein, *J. Mech. Phys. Solids* **58**, 227 (2010).
- [37] B. Noble, *Methods Based on the Wiener-Hopf Technique for the Solution of Partial Differential Equations*, International Series of Monographs in Pure and Applied Mathematics, Vol. 7 (Pergamon Press, New York, 1958).
- [38] D. S. Fisher, *Phys. Rep.* **301**, 113 (1998).
- [39] C. M. Dafermos, *Hyperbolic Conservation Laws in Continuum Physics* (Springer, New York, 2005).
- [40] L. Truskinovsky, *J. Appl. Math. Mech.* **51**, 777 (1987).
- [41] O. Kresse and L. Truskinovsky, *J. Mech. Phys. Solids* **51**, 1305 (2003).
- [42] M. Peyrard and A. R. Bishop, *Phys. Rev. Lett.* **62**, 2755 (1989).
- [43] R. Burridge and J. Keller, *SIAM Rev.* **20**, 31 (1978).